U. S. Geological Survey.

REPORTS-OPEN FILE SERIES, no. 1550: 1971.

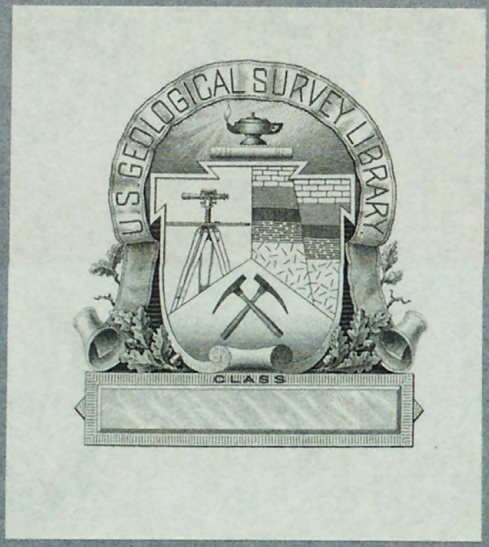
U.S. GEOLOGICAL SURVEY LIBRARY
CLASS

UNITED STATES
DEPARTMENT OF THE INTERIOR
GEOLOGICAL SURVEY

MICROEARTHQUAKE ACTIVITY IN THE VICINITY OF WOODED ISLAND, HANFORD REGION, WASHINGTON

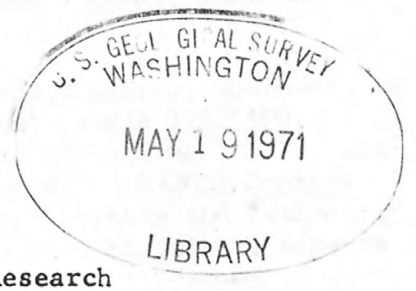

by
Andrew M. Pitt
National Center for Earthquake Research
Menlo Park, California

Prepared on behalf of the Richland Operations Office
U.S. Atomic Energy Commission

U. S. Geological Survey
OPEN FILE REPORT
This report is preliminary and has not been edited or reviewed for conformity with Geological Survey standards and nomenclature.

Menlo Park, California
1971

Weld - Int. 2905

U.S. GEOLOGICAL SURVEY
WASHINGTON, D. C.
20242

For release MAY 17, 1971

The U.S. Geological Survey is releasing in open file the following reports. Copies are available for inspection in the Geological Survey Libraries, 1033 GSA Bldg., Washington, D.C. 20242; Bldg. 25, Federal Center, Denver, Colo. 80225; and 345 Middlefield Rd., Menlo Park, Calif. 94025. Copies are also available for inspection at other offices as listed:

1. Preliminary geologic map of western Sonoma County and northernmost Marin County, California, compiled by M. C. Blake, Jr., Robert H. Wright, and Carl M. Wentworth. Map, index, explanation (total, 5 sheets), scale 1:62,500. 504 Custom House, San Francisco, Calif. 94111; 7638 Federal Bldg., Los Angeles, Calif. 90012; California Div. Mines and Geology, Ferry Bldg., San Francisco, Calif. 94111; and State Office Bldg., 107 So. Broadway, Los Angeles, Calif. 90012. /Material from which copy can be made at private expense is available in the USGS offices listed above, in San Francisco, Los Angeles, and Menlo Park, Calif./

2. Aeromagnetic map of the Stillwater complex and vicinity, south-central Montana, by the U.S. Geological Survey. Map (2 sheets), scale 1:62,500. 1012 Federal Bldg., Denver, Colo. 80202; 8102 Federal Office Bldg., Salt Lake City, Utah 84111; 678 U.S. Court House Bldg., Spokane, Wash. 99201; Montana Bureau of Mines and Geology, Montana College of Mineral Science and Technology, Butte, Mont. 59701. /Material from which copy can be made at private expense is available in the Spokane office listed above./

3. Microearthquake activity in the vicinity of Wooded Island, Hanford region, Washington, by Andrew M. Pitt. 24 p., 7 figs., 2 tables.

4. Coal reserves of Colorado tabulated by bed, by Edwin R. Landis and George C. Cone. 3 p., plus 515 tables. 1012 Federal Bldg., Denver, Colo. 80202. Colorado Geol. Survey, 254 Columbine Bldg., 1845 Sherman St., Denver, Colo. 80203.

Correction in scale: Scale was incorrect in the Apr. 26 announcement of an open-file report--Preliminary geologic map of the Funeral Mountains in the Ryan quadrangle, Death Valley region, Inyo County, California, by James F. McAllister. The correct scale of this open-file map is 1:31,680.

Introduction

The U.S. Geological Survey (U.S.G.S.) began to monitor microearthquake activity in the region of the Atomic Energy Commission's Hanford Reservation in south-central Washington in March 1969. The Division of Reactor Development and Technology (DRDT), of the Atomic Energy Commission (AEC), supported the operation of a network of 6 (later 7) short-period, high-gain seismograph stations (Figure 1) through June 1970. Then the Chemical Processing Division (CPD) of the AEC assumed support of the original 7-station network and added 9 additional stations (Figure 1). Some preliminary results from the 7-station network covering the period 23 March 1969 to 31 December 1969 were released in the U.S.G.S. open-file report "Geologic Investigation of Faulting in the Hanford Region, Washington", by James W. Bingham, Clark J. Landquist, and Elmer H. Baltz. Preliminary reports on the results from the seismograph network for 1970 have been submitted to the AEC. This report covers a specific zone of microearthquake activity located near Wooded Island in the Columbia River, which flows along the east side of the Hanford Reservation (Figure 1). The data cover the period 23 March 1969 to 28 February 1971.

Figure 1. Hanford Region of south central Washington with the U.S. Geological Survey seismograph network indicated by triangles. Solid triangle stations began operating in March 1969 (except Station A which began operating in August 1969), open triangle stations began operating in July 1970, and broken-sided triangle stations L and P began operating in November 1970. Station P was shifted to the Station D location in February 1971. Some pertinent geologic structures of the region from the U.S. Geological Survey report, "Geologic Investigation of Faulting in the Hanford Region Washington", by James W. Bingham, Clark J. Londquist, and Elmer H. Baltz are shown.

Considerations in Locating Earthquakes

These comments refer to locating earthquakes with an array of seismographs with a station spacing of about 10 to 20 km, where the earthquakes occur within or close to the network, and where the seismic waves travel entirely within the earth's crust. In this situation, the P-waves, which are the waves with the highest velocity of propagation, are considered to be somewhat more useful for location purposes than the S-waves. The arrival of S is usually more difficult to identify than the arrival of P, and the propagation velocity of S is usually less well known than that of P.

The precision with which an earthquake can be located in 2 dimensions (epicenter) and in 3 dimensions (hypocenter) is dependent upon the following factors: the number of seismograph stations recording the earthquake, the distribution of seismograph stations relative to the earthquake, the precision with which the arrivals of the seismic waves can be timed, and the accuracy of the "model" which is the assumed relationship of the velocity of propagation of seismic waves with depth that is used to compute the traveltime and travel path of the seismic waves from the earthquake to the stations of the network.

If the earthquake is within or close to the seismograph network and the station distribution is adequate, P-wave arrivals at 3 stations will give an epicenter, and P-wave arrivals at 4 stations will give a hypocenter. However, an earthquake location solution based on arrivals at 3 or 4 stations has no redundancy with which to test the reliability of the solution or to expose errors in the model. When arrivals at 5 or more stations are used to determine the earthquake location, it is possible to statistically

evaluate the location solution. As readings from additional stations are added, the statistical tests improve.

Figure 2 shows the relationship of the Wooded Island microearthquake zone to the seismograph network. The zone is near the center of a nearly equilateral triangle formed by stations B, E, and G where the P-wave traveltimes to the 3 stations are between 3 and 5 seconds. This is a geometrically advantageous situation which makes epicentral errors of less than 5 km easy to detect. However, systematic errors caused by variations in traveltime with azimuth cannot be detected, and the accurate determination of the depth of focus for an event within about 15 km of the surface would be difficult. Adding the P-wave arrival time at station O would help detect epicentral errors due to azimuthal variations in traveltime but the depth of focus would still be uncertain. To determine accurately the depth of focus of an earthquake, it is generally necessary to have at least one station with an epicentral distance less than the depth of focus of the earthquake. Thus, placing station I (and later station D) close to the Wooded Island zone greatly increased the reliability of focal depth determination.

The quality of the P-wave arrival at a seismograph station is dependent upon the size of the earthquake, the epicentral distance to the earthquake, the background noise level at the station, and the three dimensional relationship of the station to the fault causing the earthquake. With the U.S.G.S. seismograph system, a sharp P-wave arrival can be timed with an uncertainty of less than 0.05 sec. When the first half-cycle or whole cycle of P is weak, the timing uncertainty is about 0.1 sec at the frequency range of P-wave energy from local earthquakes (generally 5 to 10 cycles per

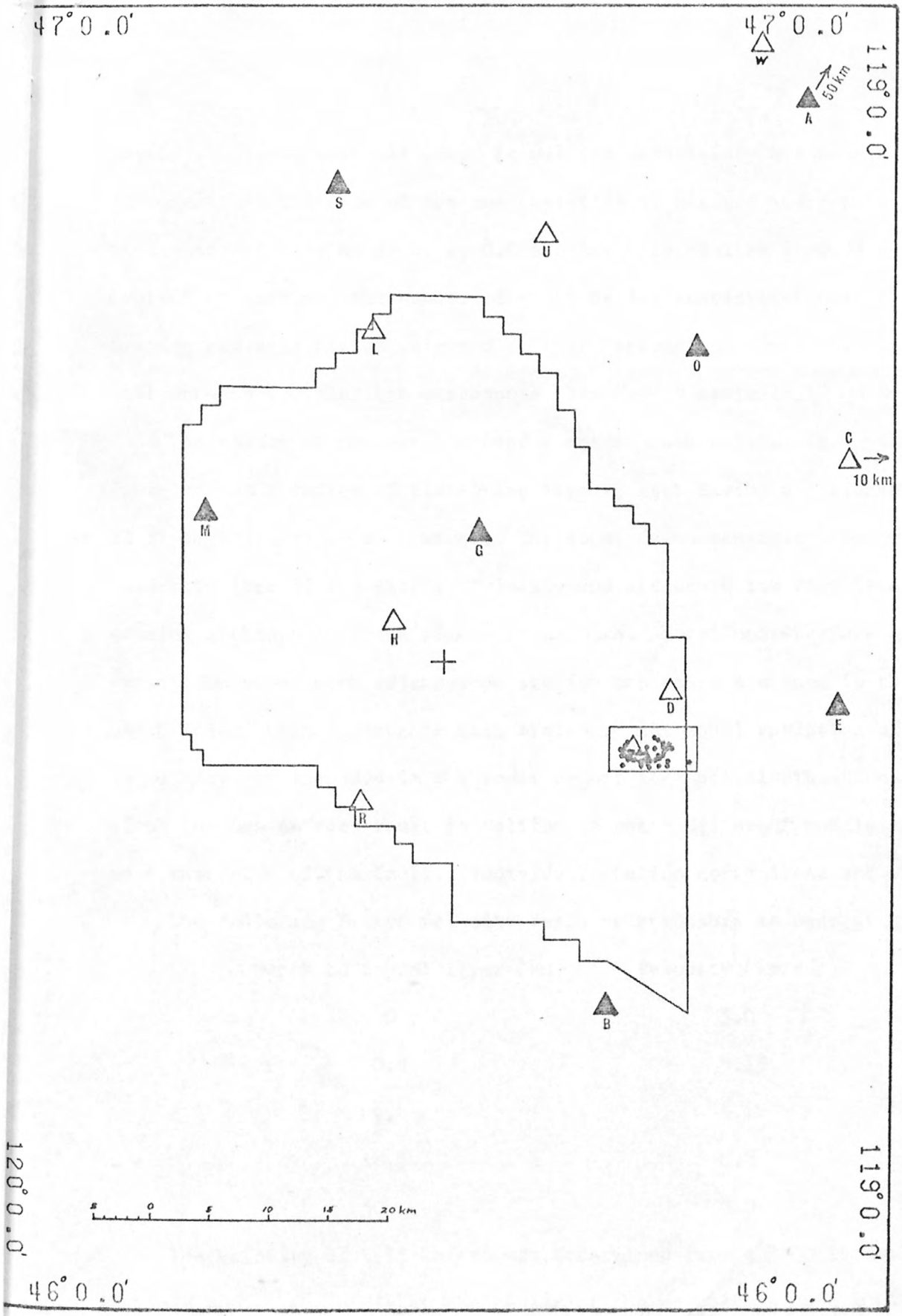

Figure 2. The irregular line is the approximate boundary of the Hanford Reservation, the solid triangles indicate seismograph stations in operation before July 1970, the open triangles indicate seismograph stations added after July 1970, and the small circles within the rectangle around station I indicate the epicenters of the Wooded Island microearthquakes. The rectangle indicates the area covered by detailed plots of the epicenters.

second). P-wave arrivals timed to 0.1 sec uncertainty are considered good for a network the size of the one operating at Hanford and P-wave arrivals with uncertainties as great as 0.5 sec may be useful to improve azimuthal control or increase the number of stations for statistical analysis. Station arrivals can be weighted so that "strong" arrivals have more influence on locating the earthquake than "weak" arrivals.

The region of the earth around a seismograph network is usually "modeled" as a series of flat-lying layers, each having a different velocity of propagation of seismic waves. The model is an approximation of the real structure of the earth. Velocity and structure can vary laterally causing a change in traveltime with azimuth. Local near-surface geologic variations under each seismograph station can cause a change in the velocity-depth relationship unique to each station. Azimuthal variation of velocity is usually not included in the model except for special situations such as along the San Andreas fault in California where different models are used on either side of the fault. Individual station corrections are often used.

The following P-wave velocity-depth relationship is used at Hanford:

Depth to top of layer (km)	Velocity (km/sec)
0	3.0
0.4	5.15
7.4	6.1
18	6.8
30	8.0

The velocity of 5.15 km/sec was determined from a 3000 lb explosion set off on GableMountain at the center of the network in June 1969. All other velocities and all layer thicknesses are assumptions based on

knowledge of crustal structure elsewhere in Washington and Idaho. Currently, large quarry shots in the Hanford Region are being used to improve the accuracy of the model.

The traveltime and travel path of the seismic waves from the earthquake to the stations of the seismograph network are computed from the model and used to "locate" the earthquake. Differences between the observed and computed arrival times at the stations are called "residuals" and can be due to model errors, individual station velocity variations, and timing uncertainties. The residuals, the number of stations, and the station distribution are all used to evaluate the accuracy of the earthquake location.

The level of activity in the Wooded Island microearthquake zone is shown in Figure 3. No microearthquakes were detected during the first 2 months of operation of the network, and the number of microearthquakes per week fluctuated by more than an order of magnitude during the 21 months following the onset of activity. The smallest microearthquakes that can generally be detected above background noise levels at stations B, E, and G have Richter magnitudes of 0. When station I was installed on top of the Wooded Island zone, microearthquakes much smaller than magnitude 0 could be detected but the level of activity in Figure 3 continued to be based on events large enough to be detected at stations B, E, and G. The largest microearthquake in the Wooded Island zone had a magnitude of 2.5 (footnote 1), and most of the events of magnitude 2 or greater occurred during the first 3 months of activity.

Epicenters were determined for 72 of the Wooded Island microearthquakes (Table 1 and Figure 4) using P-wave arrivals at between 3 and 15 stations. To examine the migration of activity with time, the epicenters were divided into successive groups of 12 events each (Figure 5).

Footnote 1:
Previously reported magnitudes for events occuring through June 1970 have been revised upward by 0.7. Magnitudes for events occurring after June 1970 are unchanged. The reason for this revision and a general discussion of the determination of magnitudes of microearthquakes will be included in the open file report on the operation of the 7-station network.

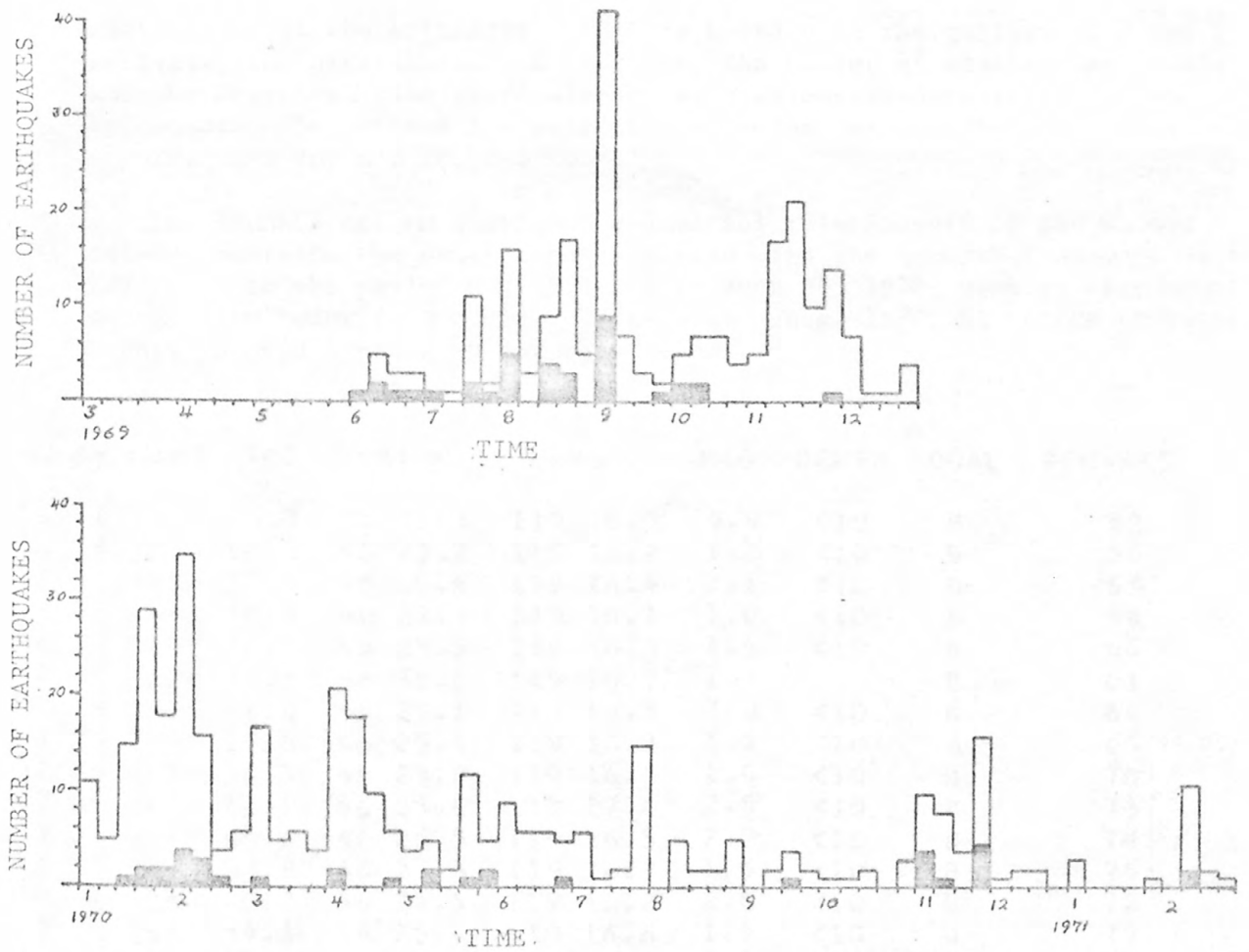

Figure 3. Level of microearthquake activity in the Wooded Island zone; time division is by week with the numbers indicating the month beginning in that week. Open bars indicate events detected and solid bars indicate events for which epicenters could be determined.

Table 1. WOODED ISLAND EARTHQUAKES - JUNE 1969 TO FEB 1971

Further small adjustments may be made in the epicenters of these earthquakes as more accurate knowledge of the crustal structure in the Hanford Region is obtained. Origin time is given in Greenwich Mean Time; MAG is Richter magnitude, DEPTH is in kilometers; and QUAL indicates the reliability of the epicenter. QUAL is based upon the quality of P and S arrivals, the distribution of stations, the number of stations available, and the P-arrival time residuals at the stations used to determine the epicenter. The letters indicate the following maximum probable epicentral errors: A-1 km, B-3 km, C-5 km.

The REMARKS column shows the sequential relationship of the Wooded Island events to the other events located with the network. Numbers 52 to 279 refer to the period May 23, 1969 to June 30, 1970; numbers with month designation refer to monthly reports after June, 1970; EX refers to extra events located especially for this report.

IM	MO	DY	HRMN	SEC	LAT N	LONG W	MAG	DEPTH	QUAL	REMARKS
1	6	1	1216	45.0	46 25.3	119 16.7	0.9	<10	B	52
2	6	8	1236	12.3	46 25.2	119 16.2	1.2	<10	B	56
3	6	10	1450	27.3	46 25.4	119 16.4	2.1	<10	B	57
4	6	15	453	36.4	46 25.3	119 16.1	1.0	<10	B	58
5	6	27	241	20.3	46 25.5	119 16.3	1.4	<10	B	60
6	7	1	622	38.2	46 25.6	119 16.7	1.2		B	61
7	7	15	430	1.0	46 25.1	119 15.5	2.0	<10	B	64
8	7	15	2354	10.5	46 25.4	119 16.3	1.8	<10	B	65
9	7	24	1013	36.3	46 25.3	119 16.3	1.6	<10	B	70
10	7	31	614	22.1	46 25.4	119 17.0	2.5	<10	B	73
11	7	31	21 9	45.6	46 25.5	119 16.5	2.0	<10	B	74
12	8	1	1036	52.8	46 25.3	119 16.3	1.5	<10	B	75
13	8	1	1248	20.2	46 25.6	119 16.2	2.0	<10	B	76
14	8	2	2141	39.1	46 25.4	119 16.6	1.7	<10	B	79
15	8	11	550	15.6	46 25.5	119 15.7	1.7	<10	B	86
16	8	12	1418	3.1	46 25.5	119 16.1	1.3		B	88
17	8	15	1141	53.8	46 25.5	119 16.3	1.2		B	90
18	8	15	1623	4.1	46 25.2	119 16.7	2.2	<10	B	91
19	8	18	1850	57.3	46 25.3	119 16.1	1.2		B	93
20	8	21	148	30.0	46 25.7	119 16.9	1.3		B	94
21	8	22	844	1.5	46 25.4	119 14.9	1.8	<10	B	95
22	8	31	252	28.1	46 25.6	119 16.7	0.9	<10	B	96
23	8	31	1118	7.7	46 25.7	119 16.9	2.3	<5	B	97
24	8	31	1119	31.3	46 25.4	119 17.2	2.2	<10	B	98
25	9	1	035	48.0	46 25.4	119 16.8	1.2	<10	B	100
26	9	1	2027	43.2	46 25.4	119 16.8	0.9	<10	B	101
27	9	2	034	10.3	46 25.2	119 16.1	1.8	<10	B	102
28	9	2	1241	52.5	46 25.9	119 16.8	1.9	<10	B	103
29	9	4	1817	11.3	46 25.5	119 15.5	1.8	<10	B	105
30	9	6	2228	34.9	46 25.5	119 15.5	1.9	<10	B	106

Table 1. (cont.)

JM	MO	DY	HRMN	SEC	LAT N	LONG W	MAG	DEPTH	QUAL	REMARKS
31	9	21	1021	21.1	46 25.9	119 16.8	1.2	<10	B	110
32	10	2	214	27.5	46 26.0	119 16.3	1.7	<5	B	114
33	10	2	637	45.2	46 25.9	119 16.3	0.9	<10	B	116
34	10	6	1158	6.0	46 25.8	119 17.7	1.3	<10	B	118
35	10	6	12 4	1.3	46 25.6	119 17.5	1.3	<10	B	119
36	11	26	2231	8.7	46 25.6	119 15.6	1.3	<10	B	159
37	1	15	1326	59.1	46 26.0	119 15.8	1.1	<10	B	171
38	1	20	154	58.1	46 25.8	119 17.6	1.8	<10	B	174
39	1	24	1358	32.6	46 25.8	119 18.0	1.7	<10	B	175
40	1	30	557	49.4	46 26.3	119 15.5	1.6	<10	B	177
41	1	31	1122	17.5	46 26.0	119 14.6	1.4	<10	B	178
42	2	1	1751	50.6	46 25.8	119 16.5	1.4	<10	B	179
43	2	3	552	3.1	46 25.7	119 18.0	1.2	<10	B	180
44	2	5	118	18.9	46 25.7	119 17.5	1.9	<10	B	181
45	2	7	747	45.7	46 25.7	119 17.9	1.6	<10	B	182
46	2	8	2013	17.5	46 26.0	119 14.9	1.7	<10	B	184
47	2	11	1047	11.4	46 26.2	119 14.8	2.1	<10	B	192
48	2	12	919	33.8	46 26.3	119 17.7	1.0	<10	B	193
49	2	17	221	57.9	46 25.5	119 17.0	1.7	<10	B	200
50	3	3	158	40.1	46 25.9	119 15.2	1.5	<10	B	211
51	3	31	434	43.2	46 25.6	119 16.9	1.6	<10	B	234
52	4	4	1043	27.6	46 25.6	119 16.3	1.7	<10	B	236
53	4	25	220	36.3	46 25.5	119 16.9	1.7	<10	B	242
54	5	3	1031	26.3	46 25.6	119 15.2	1.0		B	245
55	5	8	848	29.2	46 25.8	119 17.3	1.5	<10	B	248
56	5	18	622	37.3	46 25.2	119 14.9	1.6	<10	B	253
57	5	24	1948	40.5	46 25.8	119 18.0	2.0	<10	B	258
58	5	29	1159	29.7	46 25.9	119 18.2	1.8	<10	B	260
59	6	26	1329	29.8	46 25.3	119 13.5	1.4	<10	B	279
60	9	19	250	5.9	46 25.5	119 15.7	1.1	<5	B	SEP 11
61	11	7	719	38.3	46 25.5	119 17.6	1.3	<5	B	NOV 7
62	11	7	719	44.2	46 25.5	119 17.3	1.9	<5	B	NOV 8
63	11	7	844	38.7	46 25.3	119 17.8	0.9	<10	C	NOV EX1
64	11	7	1433	22.7	46 26.0	119 17.7	1.1	<10	C	NOV EX2
65	11	14	1540	46.0	46 25.8	119 17.5	1.7	<3	A	NOV 15
66	11	22	1219	19.8	46 25.7	119 17.4	1.0	<3	B	NOV 21
67	11	27	551	49.5	46 26.5	119 15.8	1.1	<5	B	NOV 29
68	11	27	613	10.2	46 26.1	119 15.2	1.3	<5	B	NOV 30
69	11	27	739	28.0	46 25.9	119 15.2	1.3	<10	B	NOV 31
70	11	27	8 3	10.4	46 26.0	119 15.3	0.9	<10	B	NOV 32
71	2	12	2229	34.9	46 26.4	119 15.7	0.9	<10	C	FEB EX1
72	2	13	154	52.4	46 26.4	119 15.6	0.9	<10	C	FEB EX2

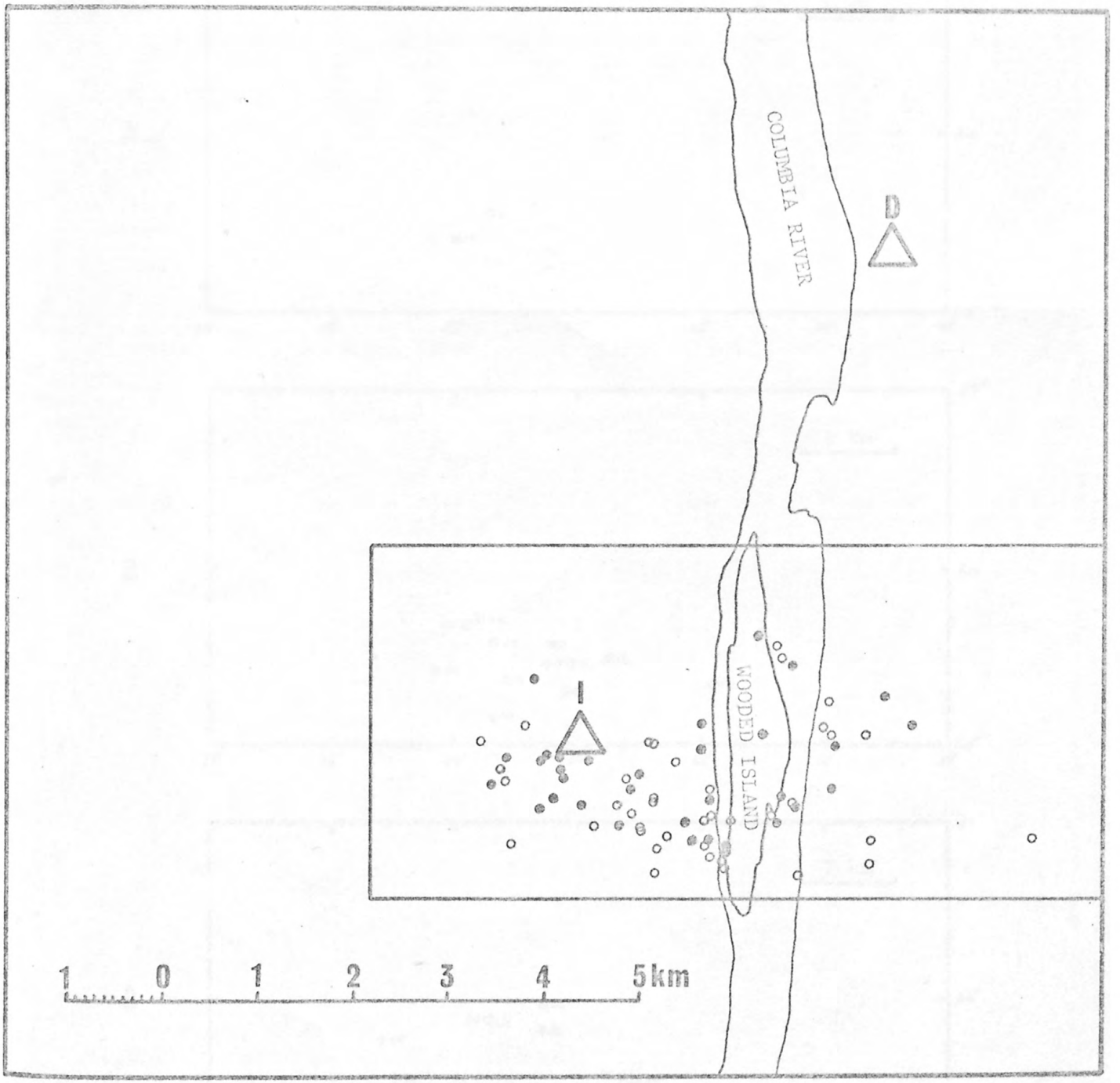

Figure 4. Enlarged view of the Wooded Island microearthquake zone; the features are the same as those described in Figure 2. Epicenters marked with solid circles are more precisely located than epicenters marked with open circles.

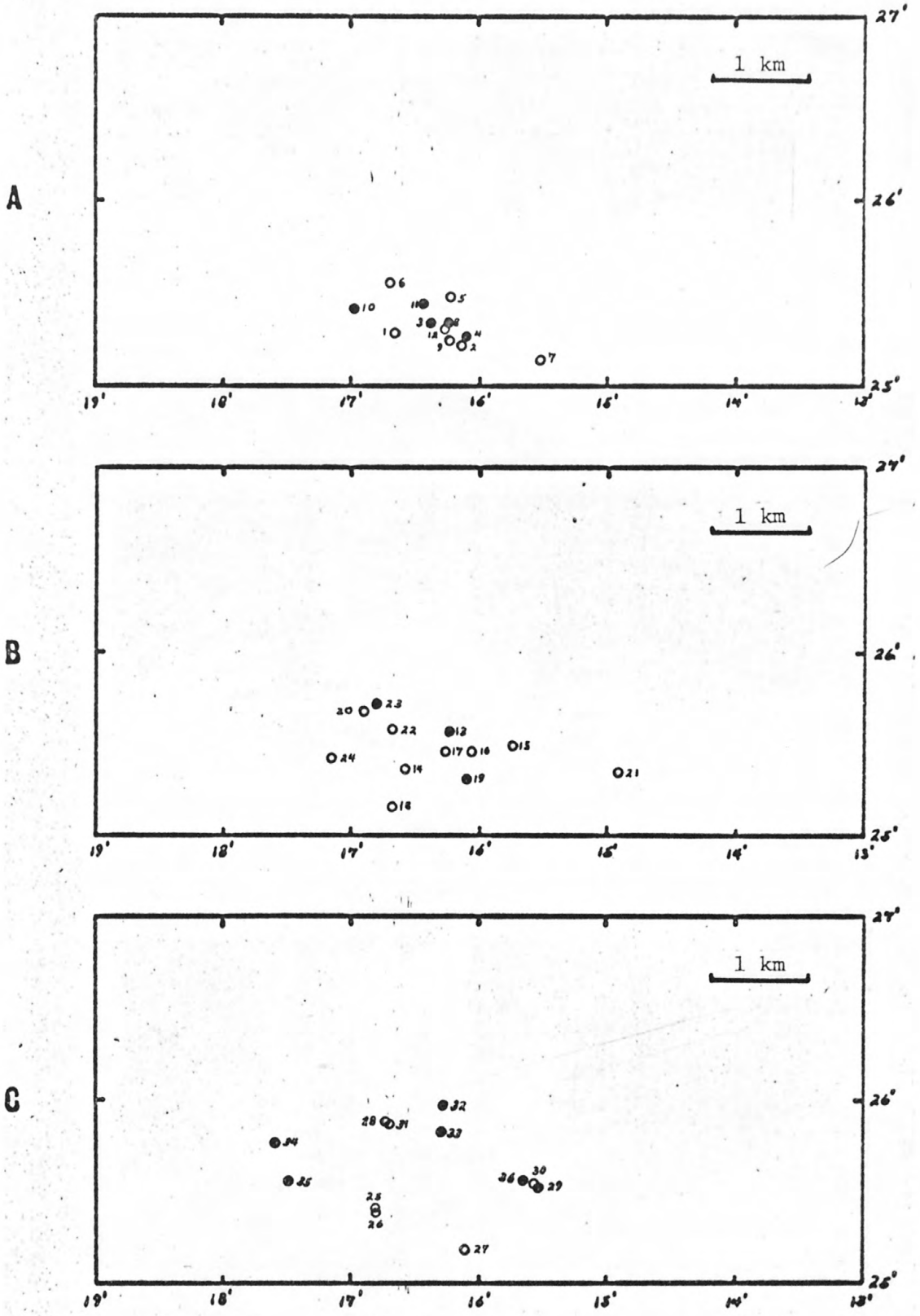

Figure 5. Progression of microearthquake activity in groups of 12 events each; epicenters marked with solid circles are more precisely located than epicenters marked with open circles. Minutes are from latitude 46°N and longitude 119°W.

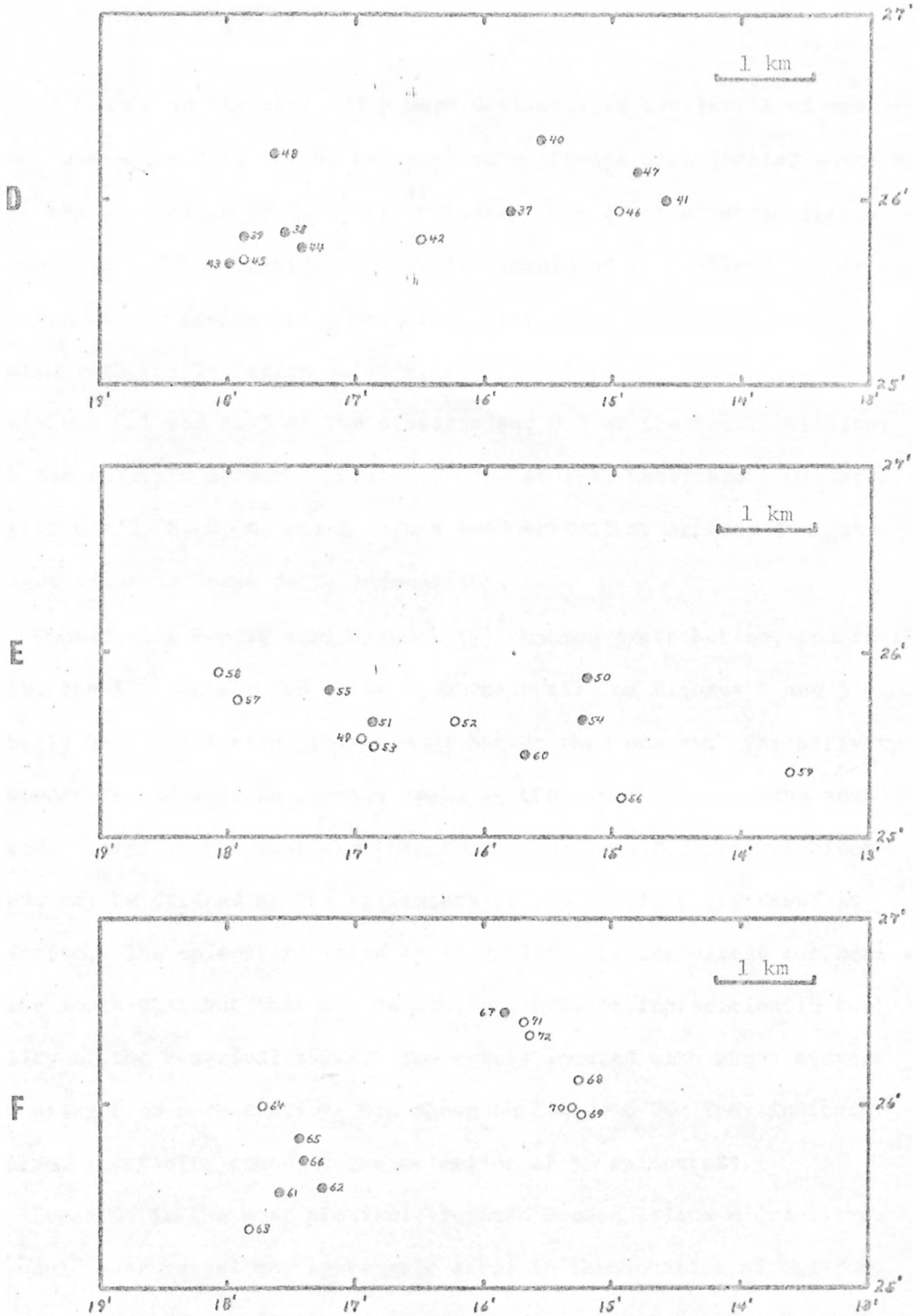

Figure 5.(continued)

The epicenters in Figures 4 and 5 were divided into two levels of precision. The epicenters marked as being more precise were located using at least the 4 stations B, E, G, and O (except for event 67 where station R was substituted for station B) and the spread of residuals at those 4 stations was no greater than 0.15 sec. For the more precise events located with the 7-station network, the acceptable P-wave arrival uncertainty was 0.1 sec at 3 of the stations and 0.2 at the fourth station. With the enlarged network, greater P-wave arrival uncertainty was accepted at stations B, E, G, O, and R when a good arrival at station I might provide valuable focal depth information.

Considering P-wave arrival quality, station distribution, and residuals, the 33 events rated as being more precise on Figures 4 and 5 probably have a relative precision of better than one km. The activity at Wooded Island appears to have begun at the center of the zone and expanded first to the west and then to the north-east. Several minor trends may be defined by the epicenters but no single major trend is indicated. The epicenters rated as being less precise extend the zone to the south-east but this may be due to a greater inprecision in the quality of the P-arrival times. Ten events located with above average data using 6 or more stations are shown on Figure 6-C. They indicate the same indefinite trend as the selection of 33 epicenters.

Event 65 is the most precisely located Wooded Island microearthquake and would best reveal any systematic error in the location of the zone. The data and solution for event 65 are shown in Table 2. The P-waves to 11 of the 15 stations used in the solution travel through the 5.15 km/sec layer (stations with ANIN $< 90°$) which is the best defined feature of the model. The P-wave arrivals and residuals at stations B, E, G, and O for

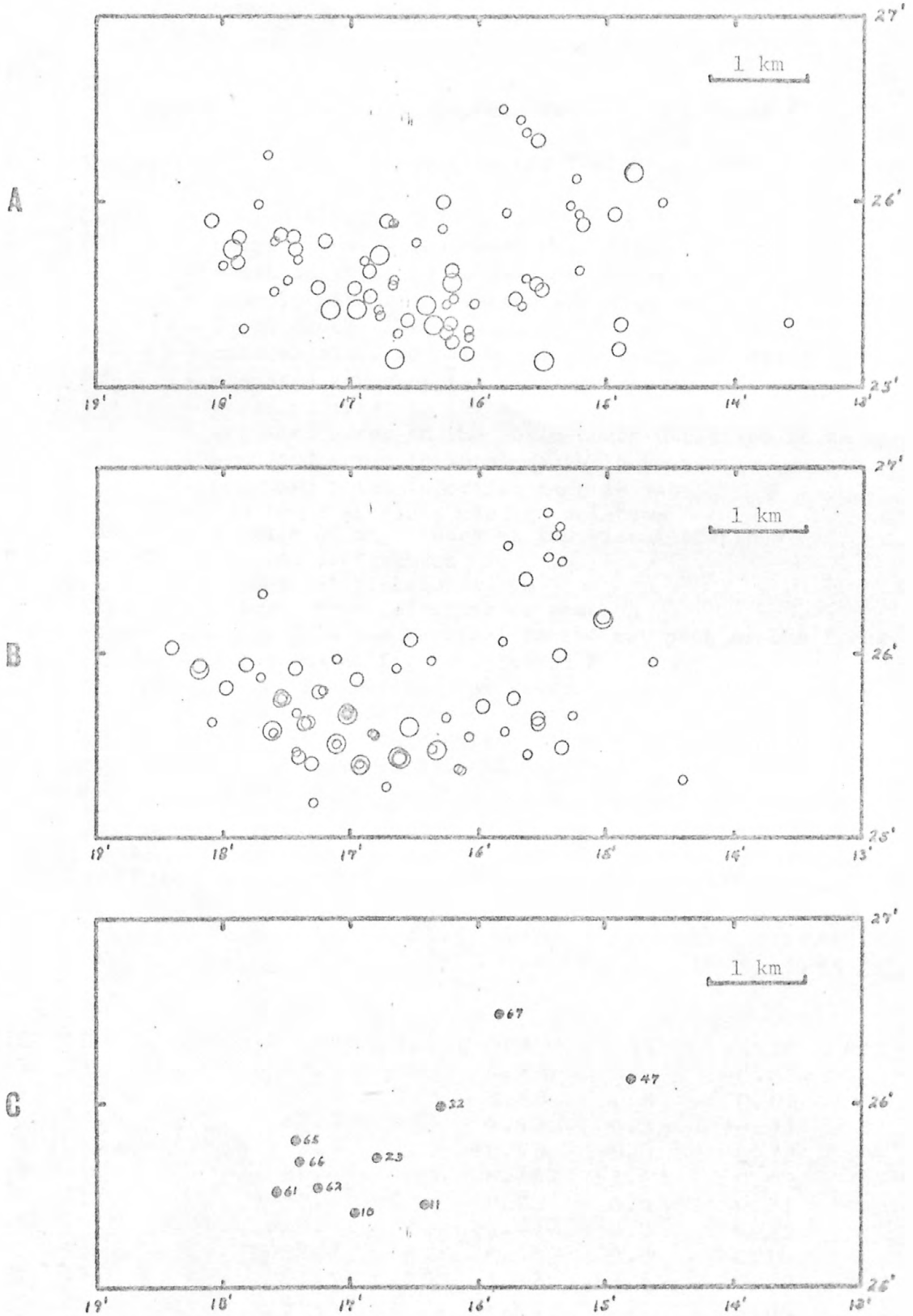

Figure 6. A and B show variation of magnitude of events: small circles - M <1.5; medium circles M 1.5 - 1.9; large circles - M ≥2.0. A epicenters are located using all possible station readings, B epicenters are located using stations B, E, and G, or E, G, and R.

C shows the epicenters of the 10 best located events.

Table 2. Data and Hypocenter Solution for Event 65

The earthquake is described with the following terms:

DATE - year-month-day
ORIGIN - origin time in Greenwich Mean Time
LAT - north latitude in degrees and minutes
LONG - west longitude in degrees and minutes
DEPTH - focal depth in km
AAF - mean absolute deviation of the P-arrival residuals
SDP - standard error of the P-arrival residuals
SDX - standard error in the east-west direction in km
SDY - standard error in the north-south direction in km
SDZ - standard error in focal depth in km
SDT - standard error in origin time in sec
KSTA - number of stations used in solution
XMAG - average of magnitudes at individual stations
STATION - station designation
DELTA - epicentral distance in km
AZI - azimuth from epicenter to station
ANIN - angle from the vertical to the ray path at the focus
QSABE - direction of first motion of P
TP - observed traveltime of P-wave
TS - observed traveltime of S-wave
RESID - residual - observed time minus computed time
MAG - magnitude at individual stations
W - weighting factor for P-wave arrival

DATE	ORIGIN	LAT	LONG	DEPTH
701114	1540 45.97	46. 25.84	110. 17.50	1.4

AAF	SDP	SDX	SDY	SDZ	SDT	KSTA	XMAG
0.11	0.18	0.5	0.5	0.9	0.07	15	1.74

STATION	DELTA	AZI	ANIN	QSABE	TP	TS	RESID	MAG	W
B	21.8	185.	97.4	PU	4.38	0.0	-0.02		1.00
E	18.3	73.	96.9	PD	3.68	0.0	0.03		1.00
G	22.6	325.	87.5	IPD	4.43	0.0	-0.11		1.00
A	105.8	23.	122.4	P	18.53	0.0	-0.28	2.08	0.25
O	34.7	10.	98.4	PD	6.78	12.43	0.03		0.75
M	41.3	299.	98.7	EP	8.23	0.0	0.21		0.25
S	54.1	333.	122.4	EP	10.43	0.0	0.25		0.25
L	41.9	329.	98.7	P	8.33	0.0	0.10		0.25
C	37.9	49.	98.5	PD	7.53	13.13	0.07		0.75
R	23.2	253.	97.6	IPD	4.53	0.0	-0.04		1.00
H	23.0	299.	97.6	P	4.63	9.13	0.06	1.23	0.50
I	0.3	57.	14.8	IPU	0.33	0.0	0.01		1.00
U	44.4	350.	98.7	P	8.63	16.33	-0.10	1.96	0.50
V	79.1	318.	122.4	EP	14.73	0.0	0.30	1.96	0.25
W	60.9	11.	122.4	P	11.33	0.0	-0.12	1.56	0.50

event 65 meet the criteria used to select the 33 more precise events on Figures 4 and 5. Thus the solution for event 65 does not discredit the solutions based on a smaller number of stations.

As a further test of whether the wide variation in the number of stations used to determine the epicenters influenced the shape of the Wooded Island zone, all events were located (Figure 6-B) using only stations B, E, and G or E, G, and R (events 67 to 70). The focal depth was fixed at 1.5 km based on the depth of event 65. While the position of some of the events considered to be less precisely located shifted up to one km (event 59), the shape of the zone remained essentially the same. The overall shift of the zone to the north could be due to a higher-velocity travel path to station G or a lower-velocity travel path to station B which could not be detected in a solution based on 3 stations. To test whether the shift of events 67 to 70 to the north could be due to the substitution of station R for station B, event 65 was located with both three-station combinations. The 2 locations varied by only 0.4 km while event 67 is 2 km from event 65. The northward shift of the later events appears to be genuine.

The epicenters were divided into 3 ranges of magnitude in Figures 6-A (epicenters same as in Figure 4) and 6-B (3 station epicenters). There appears to be no concentration of higher magnitude events in any part of the zone.

Accurate focal depths could not be determined for most of the Wooded Island microearthquakes due to station distribution but for those events where focal depth control was available, depths were all less than 5 km. Event 65 had a focal depth of 1.5 km with a possible depth error of less than one km.

Magnitude Distribution

The magnitude distribution of earthquakes has sometimes been used to estimate recurrence intervals of large magnitude shocks. Allen et al. (1965) showed that the technique works fairly well for southern California as a whole, but that it does not yield proper estimates for smaller regions in southern California. The magnitude distribution is usually plotted as the logarithm of the number of earthquakes above magnitude M against M. Figure 7 shows this type of plot for the Wooded Island zone. The number of located events was too small to make an adequate sample, so a method was devised to determine magnitudes for all of the events detected with the 7-station network. This gave a sample of 500 events. Whenever possible, the amplitude of the microearthquake at station M was used to determine the magnitude. The advantages of station M are: it is far enough from the Wooded Island zone to make the 4 km uncertainty in epicentral distance unimportant; it has a low background noise level so events down to about M = 0.5 can be seen; and it is far enough from the zone to see the peak amplitudes on events that are too large to be measured on closer stations. Amplitudes for events between M = 0 and M = 0.5 were read on stations O, B, or E. Several events large enough to be located but small enough to still see peak amplitudes at all stations were used to prepare curves relating magnitude to amplitude at stations M, O, B, and E. The curves were then used to compute magnitudes for all detected events.

Lines drawn through the points of a magnitude distribution commonly have slopes in the range of a few tenths on either side of -1.0. A line with this slope is drawn in Figure 7 for reference. In the magnitude range 0.5 to 1.6, a slope near -1.0 appears to be appropriate. The change in slope for magnitudes below 0.5 is probably due to smaller events going undetected

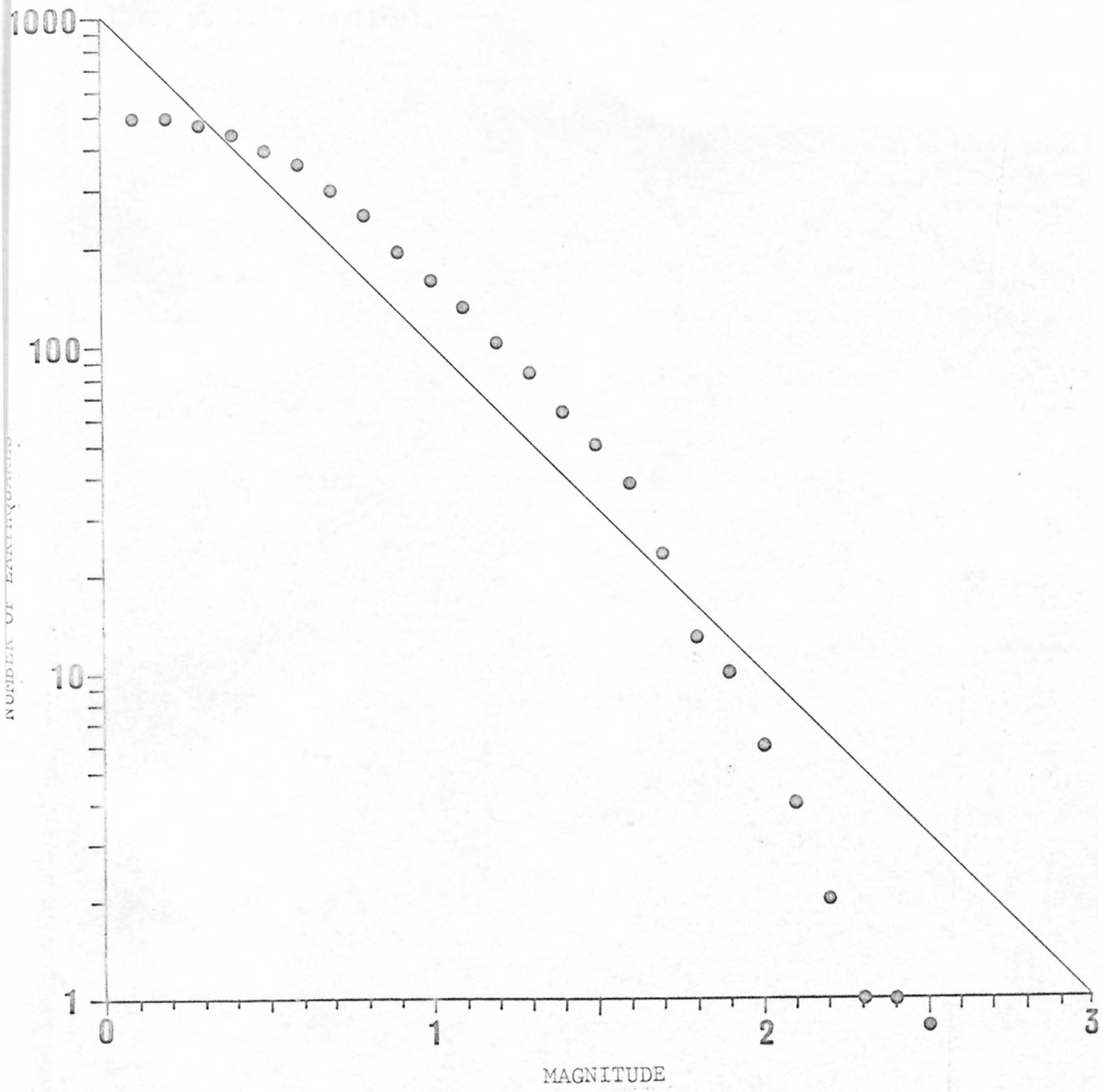

Figure 7. Number of earthquakes larger than a given magnitude versus magnitude; all Wooded Island events through June 1970 used in plot; a line with a slope of -1.0 is shown for reference.

during periods of high background noise levels. The change in slope for magnitudes above 1.6 is not readily explained but is not atypical of frequency magnitude distributions from other small regions (Eaton et al., 1970, p. 1188 and 1189).

Focal Plane Analysis

Earthquakes are caused by shear dislocations on an approximately plane surface and the direction of the first motion of P at a seismograph station is influenced by the orientation of the shear plane to the seismograph. If a sufficient number of properly distributed seismograph stations record the first motion of P from an earthquake, it is possible to learn something about the orientation of the shear plane. The first motion solution is never unique because it always defines 2 orthogonal planes, either of which could be the shear plane. Geologic investigation must be used to eliminate one of the possible planes. If the data is insufficient, more than 2 planes may be defined by the first motions of P and the uncertainty is increased.

No consistent first motion pattern has been observed at Wooded Island. No single event had more than 6 sharp first motion readings and a composite first motion plot does not yield a good solution. The shallow focal depths of the Wooded Island events complicate the calculation of the travel paths of the P-waves because of uncertainties in the velocity model.

Thus it is thought that a focal plane solution based on the current data would not aid in understanding the Wooded Island seismicity.

SUMMARY

The present data indicate that the Wooded Island microearthquakes occur in an isolated zone extending approximately 5 km from east to west and 3 km from north to south. The epicenters may define some minor trends within the zone, but no major trend is apparent. The Wooded Island events are mostly below magnitude 2 and probably less than 5 km deep. The level of activity fluctuates considerably with time.

When the current studies on the velocity-depth relationship in the Hanford region are completed, it should be possible to improve the precision of the Wooded Island epicenters and to make some focal plane studies to better understand the process causing the microearthquakes.